

# **Palaeo plant diversity in subtropical Africa – ecological assessment of a conceptual model of climate–vegetation interaction**

V. P. Groner<sup>1,2</sup>, M. Claussen<sup>1,3</sup>, and C. Reick<sup>1</sup>

<sup>1</sup>Max Planck Institute for Meteorology, Bundesstraße 53, 20146 Hamburg, Germany

<sup>2</sup>International Max Planck Research School on Earth System Modelling, Bundesstraße 53, 20146 Hamburg, Germany

<sup>3</sup>Center for Earth system research and Sustainability, Universität Hamburg, Bundesstraße 53, 20146 Hamburg, Germany

*Correspondence to:* V. P. Groner (vivienne.groner@mpimet.mpg.de)

## **Appendix A**

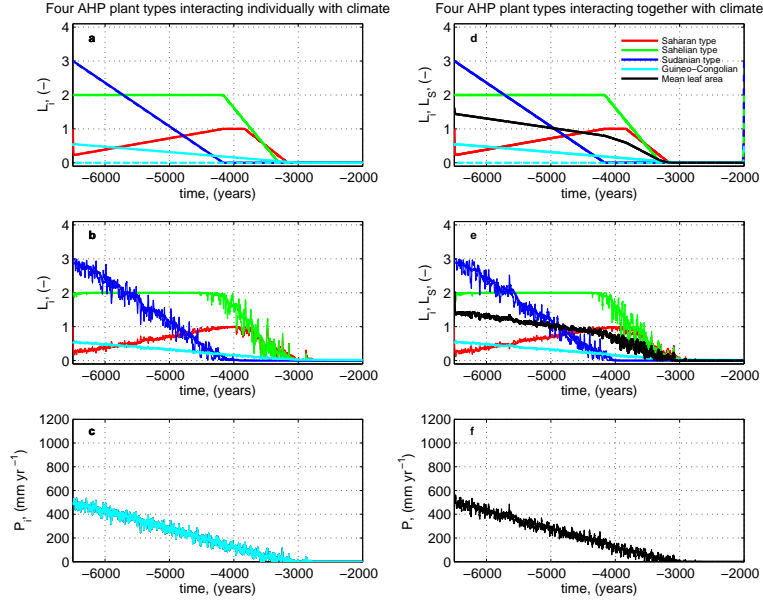


**Figure 1.** Transient dynamics of four African Humid Period (AHP) plant types interacting individually (a–c) and together (d–f) with climate for  $D_B = 0 \text{ mm yr}^{-1}$ . The effective leaf areas  $L_i$  and the corresponding precipitation amounts  $P_i$  are shown for the Saharan type (red), Sahelian type (green), Sudanian type (blue) and Guineo–Congolian type (light blue). Mean effective leaf area  $L_S$  and the corresponding precipitation  $P$  are calculated with the niche approach (black) (see Eq. 9). Simulations without background noise (a, e) include forward simulations (solid lines) and simulations backward in time (dashed lines). Simulations with background noise are depicted in (b, e) for  $L_i$  and  $L_S$ , and for precipitation  $P$  in (c, f). Thin lines show annual mean values and thick lines show a 100 year running mean.

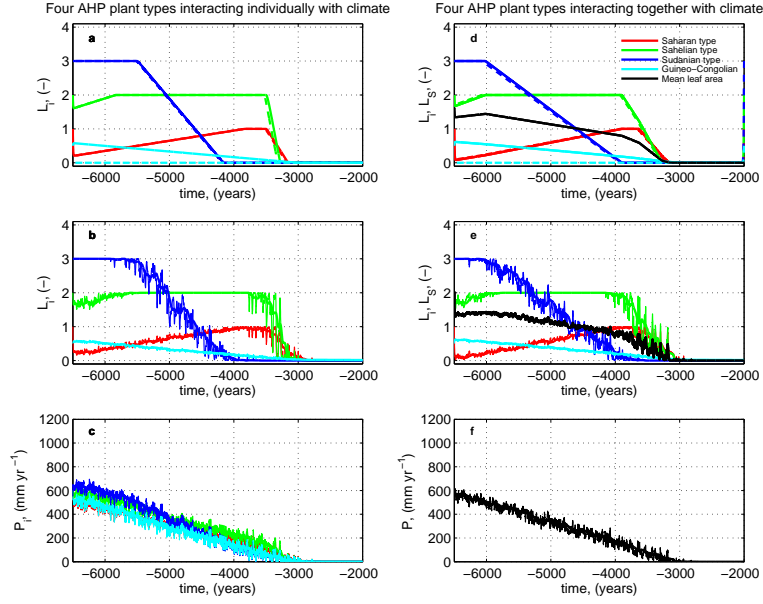


**Figure 2.** Transient dynamics of four African Humid Period (AHP) plant types interacting individually (**a–c**) and together (**d–f**) with climate for  $D_B = 50 \text{ mm yr}^{-1}$ . The effective leaf areas  $L_i$  and the corresponding precipitation amounts  $P_i$  are shown for the Saharan type (red), Sahelian type (green), Sudanian type (blue) and Guineo–Congolian type (light blue). Mean effective leaf area  $L_S$  and the corresponding precipitation  $P$  are calculated with the niche approach (black) (see Eq. 9). Simulations without background noise (**a, e**) include forward simulations (solid lines) and simulations backward in time (dashed lines). Simulations with background noise are depicted in (**b, e**) for  $L_i$  and  $L_S$ , and for precipitation  $P$  in (**c, f**). Thin lines show annual mean values and thick lines show a 100 year running mean.

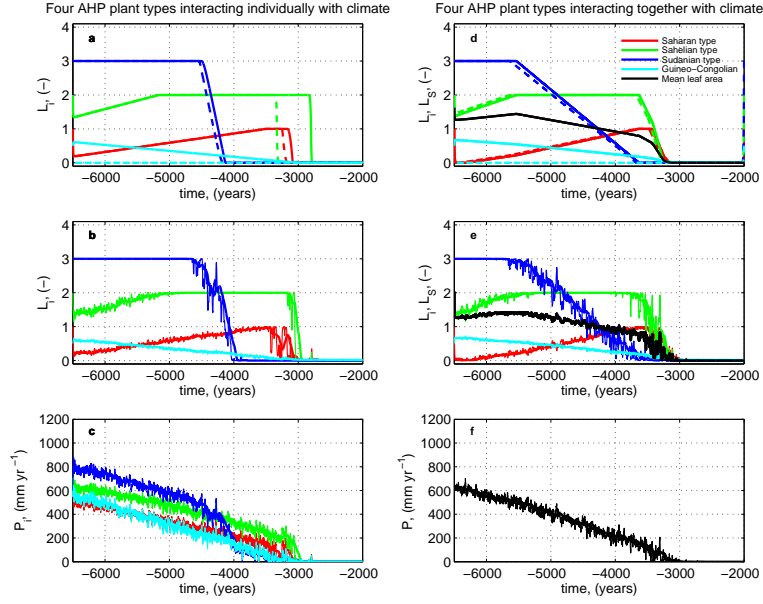


**Figure 3.** Transient dynamics of four African Humid Period (AHP) plant types interacting individually (**a–c**) and together (**d–f**) with climate for  $D_B = 100 \text{ mm yr}^{-1}$ . The effective leaf areas  $L_i$  and the corresponding precipitation amounts  $P_i$  are shown for the Saharan type (red), Sahelian type (green), Sudanian type (blue) and Guineo–Congolian type (light blue). Mean effective leaf area  $L_S$  and the corresponding precipitation  $P$  are calculated with the niche approach (black) (see Eq. 9). Simulations without background noise (**a, e**) include forward simulations (solid lines) and simulations backward in time (dashed lines). Simulations with background noise are depicted in (**b, e**) for  $L_i$  and  $L_S$ , and for precipitation  $P$  in (**c, f**). Thin lines show annual mean values and thick lines show a 100 year running mean.

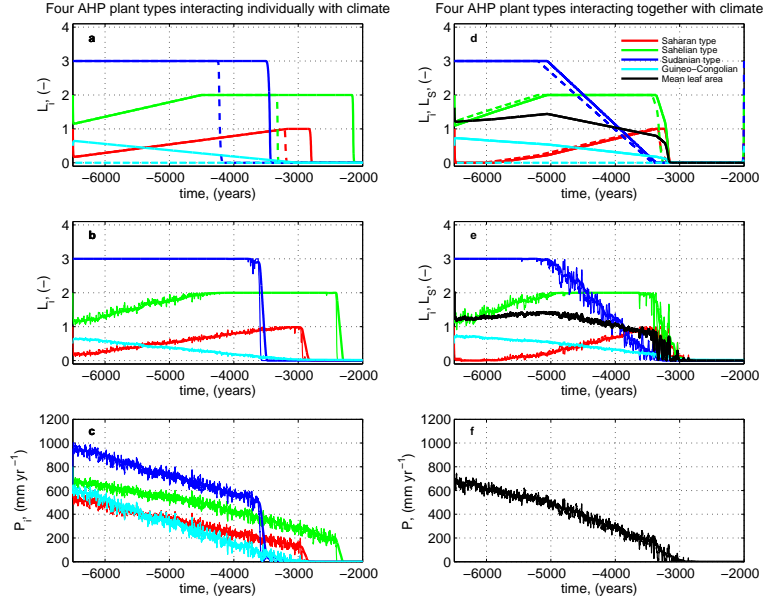


**Figure 4.** Transient dynamics of four African Humid Period (AHP) plant types interacting individually (**a–c**) and together (**d–f**) with climate for  $D_B = 150 \text{ mm yr}^{-1}$ . The effective leaf areas  $L_i$  and the corresponding precipitation amounts  $P_i$  are shown for the Saharan type (red), Sahelian type (green), Sudanian type (blue) and Guineo–Congolian type (light blue). Mean effective leaf area  $L_S$  and the corresponding precipitation  $P$  are calculated with the niche approach (black) (see Eq. 9). Simulations without background noise (**a, e**) include forward simulations (solid lines) and simulations backward in time (dashed lines). Simulations with background noise are depicted in (**b, e**) for  $L_i$  and  $L_S$ , and for precipitation  $P$  in (**c, f**). Thin lines show annual mean values and thick lines show a 100 year running mean.

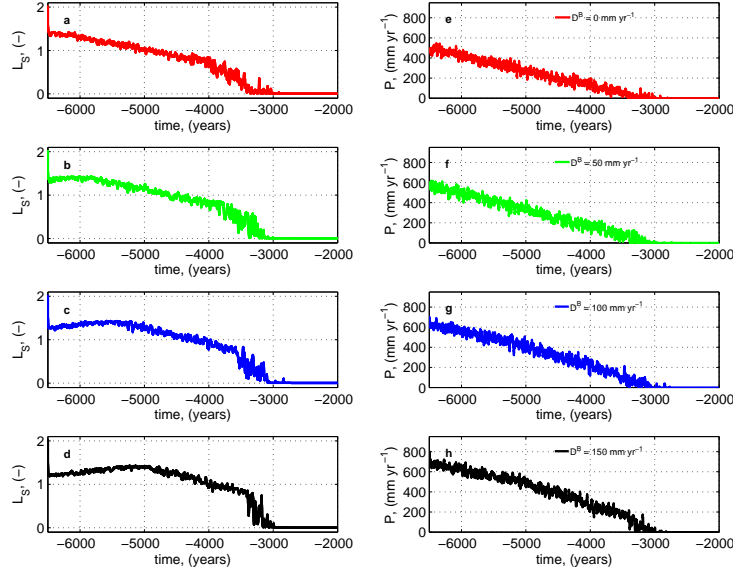


**Figure 5.** Transient dynamics of mean effective leaf area  $L_S$  of four African Humid Period (AHP) plant types interacting together with climate, and the corresponding precipitation  $P$  for different feedback sensitivity coefficients  $D^B$ . Simulations with background noise are depicted in (a–d) for  $L_S$ , and for mean annual precipitation  $P$  in (e–h) for  $D^B = 0 \text{ mm yr}^{-1}$  (red),  $D^B = 50 \text{ mm yr}^{-1}$  (green),  $D^B = 100 \text{ mm yr}^{-1}$  (blue), and  $D^B = 150 \text{ mm yr}^{-1}$  (black). Without feedback between vegetation and precipitation (a, e),  $L_S$  and corresponding  $P$  decrease almost linearly. Low feedback coefficients (b, f) result in a non-linear but gradual decline of  $L_S$  and corresponding  $P$  with small fluctuations. The higher  $D_B$ , the stronger the amplitude of fluctuations and the steeper the decline of  $L_S$  and corresponding  $P$ .

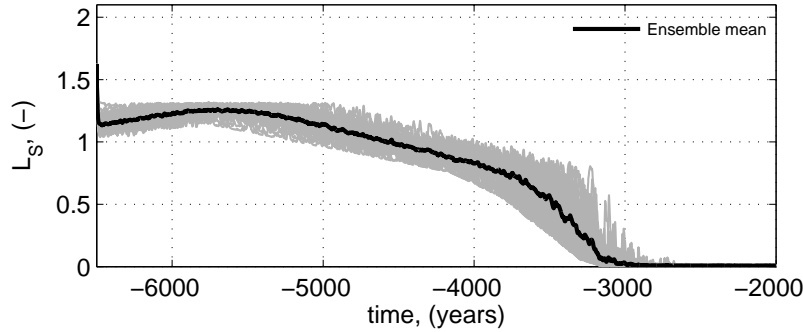


**Figure 6.** Mean effective leaf area  $L_S$  of four African Humid Period (AHP) plant types  $i$  interacting together with climate with different sets of specific climate feedback coefficients  $D_i^B$ . 30 simulations with different variations of  $D_i^B$  in the range from 0 to  $150 \text{ mm yr}^{-1}$  are shown in gray, the ensemble mean is shown in black.